Roots of coastal plants stabilize carbon fixed by marine algae

Inga Hellige[1,2], Aman Akeerath Mundanatt[1,2], Jana C. Massing[1,2] and Jan-Hendrik Hehemann[1,2*]

[1] Marum Centre for Environmental Research, University of Bremen, Germany

[2] Max-Planck Institute for Marine Microbiology, Germany

*Corresponding author. Email: jhhehemann@marum.de

Keywords: carbon dioxide removal | marine carbon sequestration | glycans | coastal vegetated ecosystems

Abstract

Coastal vegetated ecosystems are key-nature based solutions in climate change mitigations. Mangroves, seagrass meadows and saltmarshes contribute to carbon sequestration not only through the storage of biomass and sediments, but also through the secretion of dissolved organic carbon over their root system. Macro- and microalgae release most of their produced organic carbon as exudates, exported away from their origin, leading to underrepresentation of their contribution in blue carbon assessments. Here, we analysed 93 sediment cores of coastal vegetated ecosystems from temperate to tropical regions. We used polysaccharides as bioindicators of carbon sequestration to trace carbon from source to sink in different ecosystems. By binding of specific monoclonal antibodies, algal-derived polysaccharides were detected in sediments of coastal vegetated ecosystems. The relative abundance of the main building blocks of polysaccharides, monosaccharides was consistent across all 93 sediment cores, with no significant differences, despite the varying ecosystems and locations. Our findings suggest that the restoration of plant ecosystems, fixing carbon, protecting coasts and enhance biodiversity should also be enumerated for the stored carbon from distant donors.

Hence carbon sequestration is a collective or synergistic process of different photosynthetic organisms.

Significance statement

Coastal vegetated ecosystems are vital for climate change mitigation, sequestering carbon through biomass, sediments and the integration of organic carbon from external sources such as algae. By using polysaccharides as bioindicators, this study reveals that algal-derived carbon is preserved in sediment across diverse ecosystems, emphasizing the synergistic role of multiple photosynthetic organisms in carbon sequestration. This finding indicates that coastal vegetated ecosystems accept, accrete and stabilize carbon from different and distant donors and highlights the collective contribution of these ecosystems to global carbon storage.

Main

Coastal vegetated ecosystems, including mangroves, seagrass meadows, and saltmarshes, play a crucial role as carbon sinks, storing estimated amounts of up to 0.7 Pg carbon year^{-1} (1). With carbon sequestration rates up to 10 times greater than those of terrestrial forests (2), these ecosystems are increasingly recognized as nature-based climate solutions. This high carbon sequestration capacity, coupled with their abilities to protect coastlines, support biodiversity, and improve water quality, underscores their significance in carbon dioxide removal (CDR) strategies (3–5).

Mangroves, seagrass and saltmarshes sequester carbon through biomass and sediment storage and by releasing dissolved organic carbon (DOC) through their root system. Seagrass meadows were shown to be enriched in the sugar sucrose compared to unvegetated areas (6). In contrast, macro- and microalgae, which lack root systems, release most of their carbon as exudates, constituting between 1% and 35% of their net primary production (7–11). Due to the challenges in tracking algae's carbon storage potential from source to sink, they are often excluded from blue carbon strategies (12, 13).

Despite these challenges, algae contribute substantially to blue carbon pools. Macro- and microalgae have been shown to supply up to 50% of the carbon in seagrass sediments (14) and up to 60% of Red Sea mangrove sediments (15), identifying algae as significant carbon donors (12, 16). However, once release into the environment, tracking algae-derived carbon becomes complex. While a portion of this carbon is remineralized, 10-60% can persist under environmental conditions, potentially forming long-term carbon sinks (13, 17–19).

Further complicating this tracking process is the complexity of algae exudates. For instance, brown algae and diatoms secrete the complex and variable extracellular matrix polysaccharide fucoidan that might resist microbial degradation (20–24). These substances can assemble into particles (20, 25) that are carried by tides and currents before sinking to sediment (26, 27).

The extent of carbon transport and the composition of the stored organic carbon in coastal vegetated ecosystems remains understudied. Tracing carbon from source to sink is essential for understanding the potential for long-term carbon storage. Here, we hypothesized that polysaccharides can serve as bioindicators for algal carbon stored within coastal vegetated ecosystems, suggesting that blue carbon sequestration results from the collective carbon sequestration across ecological communities.

Results

Global sediment analysis revealed similar monosaccharide abundance despite different ecosystems and locations

To investigate the mono- and polysaccharides stored in sediments across coastal vegetated ecosystems, we analysed 93 sediment cores from the North Sea, Baltic Sea, Malaysia and Columbia. 50cm deep sediment cores were taken in saltmarsh, seagrass, mangroves and unvegetated areas (**Fig. 1A-C, Table S1**). Up to 3 points per ecosystem were sampled along a transect (**Fig. 1D**).

The major building blocks of polysaccharides, including fucose, galactose, glucose, mannose, xylose and galacturonic acid were found to be shared between all ecosystems and depths. Applying a non-metric multidimensional scaling (NMDS) analysis to the dataset of relative abundances of monosaccharides in each sample, we found no distinct clusters among the 93 sediment cores, indicating the composition of each sample remains unchanged with location and ecosystem (**Fig. 1E**). Diffusion mapping the dataset of relative abundances, revealed a reverse relationship between fucose and glucose, where high fucose abundances occur with low glucose abundances and vice versa (**Fig. 1F-G**).

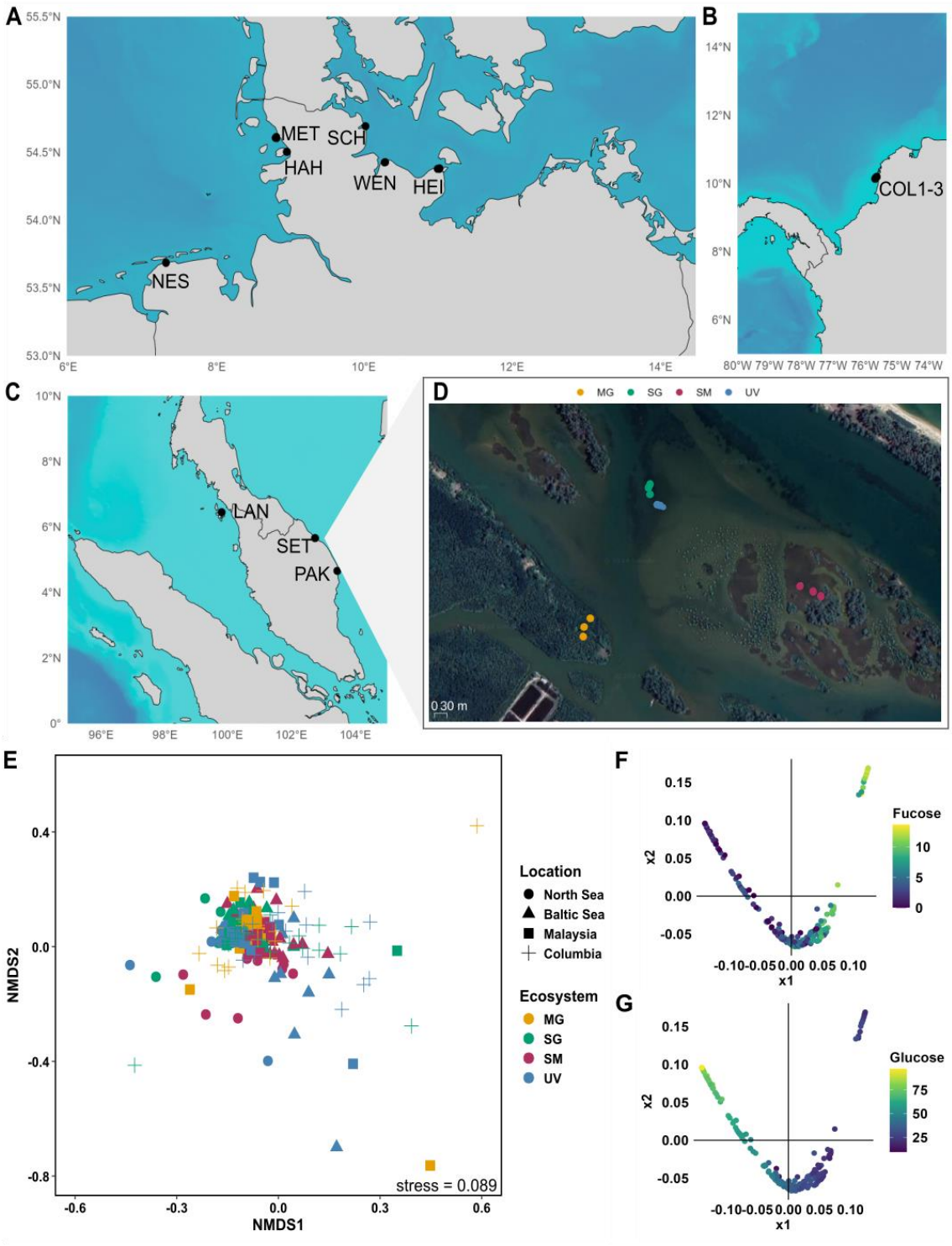

Figure 1. 93 analysed sediment cores from temperate to tropical regions revealed no major differences in monosaccharide abundances, despite diverse ecosystems and locations. A-C) Global sampling map of sediment cores of coastal vegetated ecosystems. Bathymetrie is increasing with darker blue scale, bathymetry data is from NOAA (2022), plotted with R packages 'marmap' (28) and 'sf' (29). **A)** Sampling locations along the North and Baltic Sea, Germany. NES: Nessmersiel, HAH: Hamburger Hallig, MET: Mettgrund, SCH: Schleimünde, WEN: Wendtorf, HEI: Heiligenhafen, **B)** in Columbia: COL sites 1 to 3 and **C)** in Malaysia, LAN: Langkawi, SET: Setiu, PAK: Paka. **D)** Example transect map, plotted with QGIS 3.22, of analysed transect point in ecosystems sampled in Setiu, Malaysia: mangroves (yellow), seagrass (green), saltmarsh (maroon), unvegetated (blue). Further

information on analysed sampling points with locations are shown in supplementary **table S1**. **E)** Non-metric multidimensional scaling (NMDS) plot, calculated by Bray-Curtis dissimilarity of monosaccharide composition of MilliQ-water and EDTA extracts across different sediment layers for four locations, North Sea and Baltic Sea in Germany, Malaysia and Columbia for four ecosystems, mangroves (MG, yellow), seagrass (SG, green), saltmarsh (SM, maroon) and unvegetated (UV, blue). NMDS stress level of 0.089. **F-G)** Diffusion maps of the relative abundances of monosaccharides identify new explanatory variables. X1 and x2 correspond to two new variables that identify the main dimensions of the data manifolds. Colouring the datapoints by relative abundance of fucose **(F)** and glucose **(G)** reveals an inverse relationship, where samples with high fucose levels tend to have low glucose levels, and vice versa.

The quantification of total carbohydrates across different ecosystems revealed the highest maximum mean concentrations of 1.67 ± 0.23 mg g_{dw}^{-1} in saltmarsh sediments. Mangroves and saltmarshes showed significant higher concentrations compared to seagrass and unvegetated areas ($p<0.001$) (**Fig. 2A**). Of the total carbohydrates, 10% could be attributed to total hydrolyzable carbohydrates. Except for mangroves, all ecosystems showed significant differences to each other ($p<0.001$, after Bonferroni correction, $\alpha=0.0083$) (**Fig. 2B**). Unvegetated areas ranged the lowest in mean concentrations of 35.94 ± 1.04 ug g_{dw}^{-1}, followed by seagrass with 67.65 ± 2.32 ug g_{dw}^{-1} and saltmarsh (250.55 ± 9.04 ug g_{dw}^{-1}) areas. Mangroves recorded the highest mean concentrations of 494.08 ± 45.51 ug g_{dw}^{-1}, but also the greatest variations (**Fig. 2B**).

Fucose concentrations averaged 4.60 ± 0.34 ug g_{dw}^{-1} across all samples (**Fig. 2C**). Significant differences were observed among concentrations between seagrass and unvegetated ($p= 0.0066$) and saltmarsh and unvegetated sediments ($p<0.001$, after Bonferroni correction, $\alpha = 0.0083$). Mean fucose concentrations were lowest in unvegetated areas with 2.57 ± 0.46 ug g_{dw}^{-1}, followed by seagrass with 3.88 ± 0.40 ug g_{dw}^{-1}, by mangroves with 4.35 ± 0.67 and highest in saltmarshes with 7.79 ± 0.89 ug g_{dw}^{-1} (**Fig. 2C**). An increasing trend (not significant) in the relative abundance of fucose was observed in seagrass meadows (ANOVA, $p = 0.0594$) comparing the sediment layer at the surface of each core to the deepest taken layer (**Fig. 2D**). Fucose accounted for up to 10% of hydrolyzable carbohydrates. It was significantly higher in seagrass and unvegetated areas compared to saltmarsh areas in the North Sea ($p= 0.0015$, $p= 0.0135$, respectively, Bonferroni correction, $\alpha=0.0167$), as well as saltmarsh and mangrove areas in Malaysia ($p= 0.0032$, after Bonferroni correction, $\alpha=0.0083$) (**Fig. 2E**).

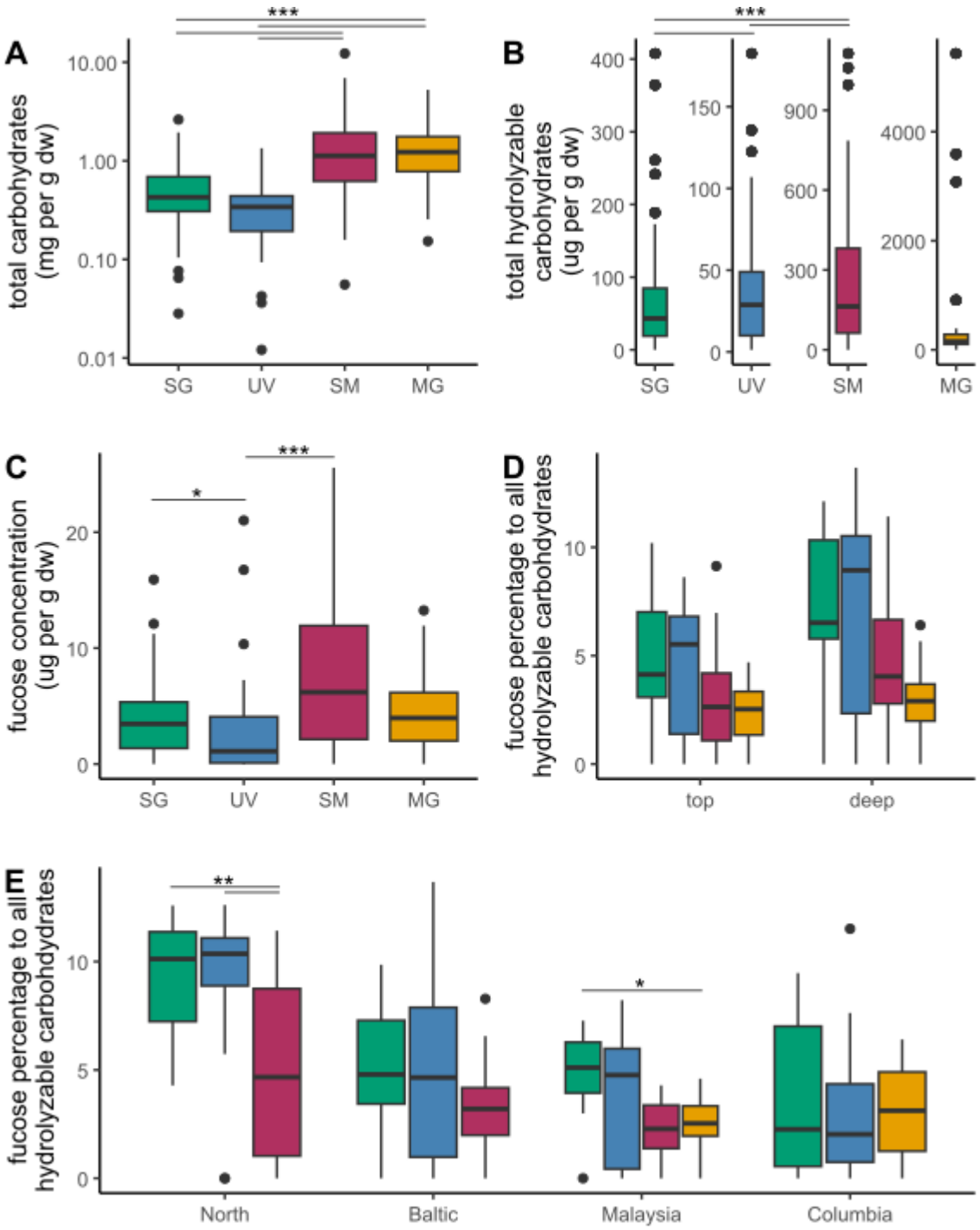

Figure 2. Up to 10% of total hydrolyzable carbohydrates can be attributed to fucose. **A)** Total carbohydrates, **B)** total hydrolyzable carbohydrates, **C)** fucose concentration in mg per g dry sediment from seagrass (SG; green), unvegetated (UV; blue), saltmarsh (SM; maroon) and mangroves (MG; yellow). **D)** Slight increase in relative fucose abundance comparing the surface layer of sediment cores to the deepest taken layer. **E)** Significantly higher fucose abundance in seagrass and unvegetated areas compared to saltmarsh sediment in the North Sea and in seagrass areas compared to mangroves in Malaysia.

Specific antibody binding shows algae glycans in sediment cores of coastal vegetated ecosystems

Structure specific monoclonal antibodies analysis indicate algae as a source of glycans in coastal vegetated ecosystems. Analysis of carbohydrate microarrays indicates the presence of alginate, pectin, fucoidan, arabinogalactan protein glycan, (1→3)-β-D-glucan and grass-xylan (**Fig. S1**). Most signals were revealed for BAM7, indicative for alginate, fucoidan or pectin, across all ecosystems in Columbia and Germany. Further JIM13 indicative for arabinogalactan-protein glycans showed signal in saltmarsh and mangrove ecosystems. Notably, the upper layer of saltmarsh cores (0 up to 9.5 cm) in Heiligenhafen (HEI), Baltic Sea, revealed signal for grass xylan (LM27), not detected in further samples (**Fig. S1**). To confirm the presence of arabinogalactans and fucoidans the more sensitive antibody method ELISA was performed. Antibody binding to arabinogalactan-protein glycan (JIM13) confirmed the signal in saltmarshes and mangroves, lower in seagrass sediments and close to no signal in unvegetated areas (**Fig. S2**). Monoclonal antibody BAM1, specific to algal polysaccharide fucoidan showed signal for all coastal vegetated ecosystems in all locations (**Fig. 3A**). Relative signal appeared to be stronger in coastal vegetated ecosystems, enriched in sediments of saltmarshes, mangroves and seagrass, slightly lower in unvegetated areas. Fucoidan stored in sediments of all coastal ecosystems was supported by the fucoidan antibody signal positively correlating with fucose concentration ($p<0.0001$ for seagrass, saltmarsh and unvegetated areas; mangroves: $p= 0.0022$) (**Fig. 3B**).

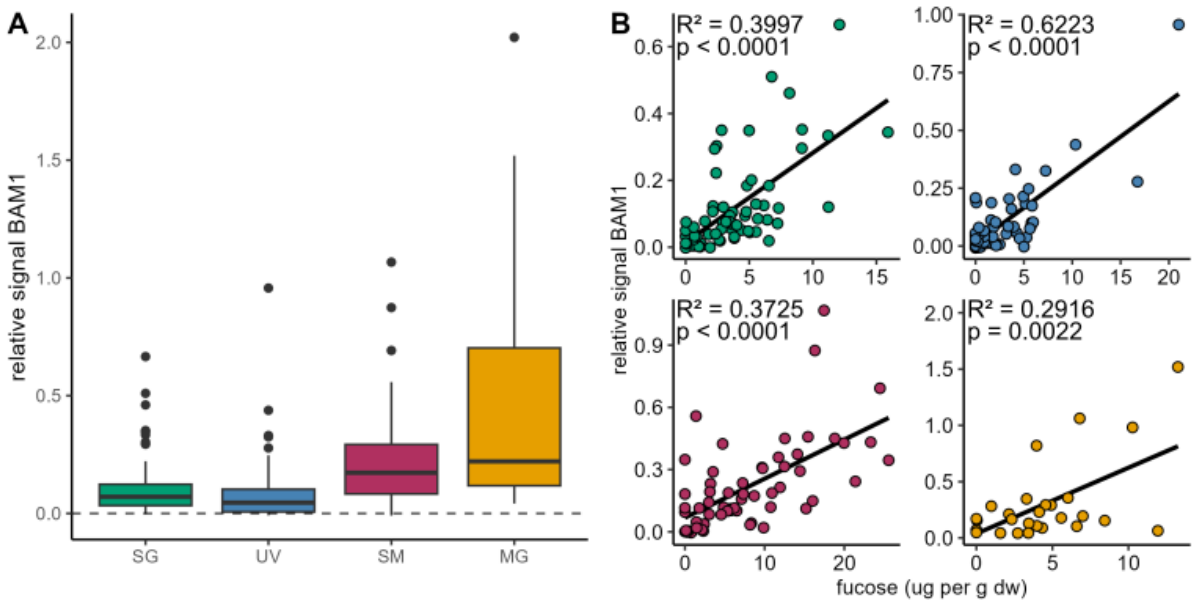

Figure 3. Algal glycan fucoidan correlates with fucose concentrations in sediments. A) Relative signal for antibody BAM1 (indicating presence of fucoidan) binding to sediment extracts from seagrass (SG; green), unvegetated (UV; blue), saltmarsh (SM; maroon) and mangrove areas (MG; yellow). Relative signal normalized to MilliQ-water blank shown by dashed line. **B)** Relative BAM1 signal correlates with fucose concentration derived from monosaccharide analysis in ug g_{dw}^{-1} (dw: dry weight).

The presence of the algal-derived glycan fucoidan was confirmed in porewater samples taken at depths of 30 to 50 cm along transects in North Sea sites (**Table S2**), using BAM1 antibody binding. The relative signal for fucoidan was notably higher beneath seagrass meadows compared to unvegetated areas. Similarly, strong signals were detected within the pioneer saltmarsh zone, relatively decreasing in within the low saltmarsh zone and being absent inside the high saltmarsh (**Fig. 4A**). These findings align with measured fucose concentrations of 46.98 ± 26.76 µg L^{-1} within the pioneer saltmarsh zone and 40.52 ± 10.85 µg L^{-1} beneath seagrass meadows. Concentrations were lower in the low saltmarsh zone (26.77 ± 11.72 µg L^{-1}) and unvegetated areas (14.56 ± 2.78 µg L^{-1}), with no detectable fucose in the high saltmarsh zone (**Fig. 4A**). These results indicate that dissolved algal-derived glycans, such as fucoidan, are secreted and transported into vegetated coastal ecosystems, which may act as acceptor systems. Algal-derived glycans carried by tidal waters may contribute to the enhancement and stabilization of sediment build-up within these ecosystems (**Fig. 4B)**.

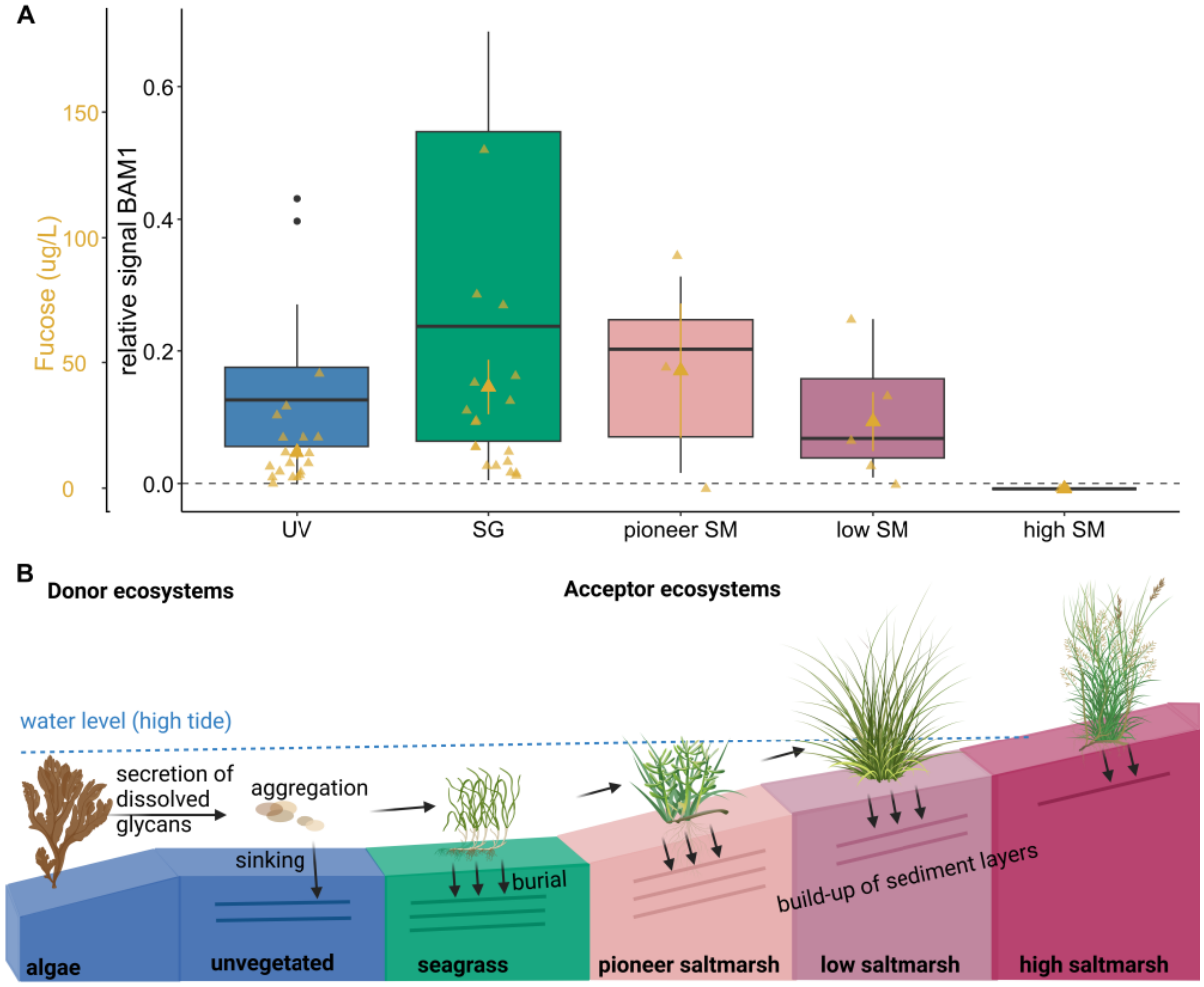

Figure 4. Algal glycan fucoidan is stored in coastal vegetated ecosystems. A) Relative signal for antibody BAM1 (indicating presence of fucoidan) binding to porewater extracts from unvegetated (UV; blue), seagrass (SG; green), pioneer, low and high (SM; rose to maroon). Relative signal is normalized to signal of MilliQ-water blank (dashed line). Mean fucose concentration in ug L^{-1} (mean ± s.e.m) for all ecosystems (yellow). **B)** Schematic view on storage of algal-derived glycans in coastal vegetated ecosystems, using BioRender (30). Donor ecosystems, such as algae secrete dissolved glycans, which may aggregate and be transported to coastal vegetated ecosystems. These acceptor ecosystems, reached by tidal waters may bury transported algal glycans and build-up of their sediment layers, accreting and storing their own and the carbon of donor ecosystems.

Discussion

This study revealed a similar monosaccharide abundance across different coastal ecosystems and study sites. We expected that dissolved organic carbon secreted by seagrass, saltmarshes and mangroves would show distinct carbohydrate profiles, according to the coastal ecosystem. However, the similarity in relative monosaccharide abundances underneath all sampled ecosystems (**Fig. 1E**) suggests a glycan continuum, as previously described in surface waters (31, 32). The only differences seem to be driven by relative

glucose and fucose abundances (**Fig. 1F-G**), indicating that fucose-rich oligosaccharides or polysaccharides might persist longer (33).

Algal-derived polysaccharides, such as fucoidan can be used as bioindicators for algal carbon sequestration, tracing sources to sinks in different ecosystems. Polysaccharide screening of sediment samples revealed most binding to alginate, fucoidan and arabinogalactan (**Fig. S1 S2, Fig.3)**. Arabinogalactan-protein glycan and fucoidan were shown to be exuded by algal species, in particular by brown algae (34). Arabinogalactan-protein glycans can additionally stem from plant sources (20, 34). Fucoidan was shown to be actively and continuously produced and secreted in the mucilage layer of brown algae and diatoms (20, 21, 25). Continuous fucoidan secretion and the resulting increase in dissolved organic matter might be followed by an increasing formation of particulate organic matter. These particles can be exported with other carbon-containing compounds through the biological carbon pump (35, 36). We showed fucoidan and arabinogalactan-protein glycan signals in coastal vegetated ecosystems, suggesting its export to and storage in coastal sediments. The enhanced abundance in coastal vegetated ecosystems reached by tidal waters compared to unvegetated areas and high saltmarsh areas (**Fig. 4**) highlights the importance of algae as donor ecosystems to blue carbon (12, 13), while roots of plants accept and stabilize carbon storage. However, the loss of at least around 7% of seagrass areas and up to 3% of saltmarsh and mangrove areas annually (2), reduces the potential for fucoidan and further algal-derived carbon sequestration in these ecosystems.

In conclusion, coastal vegetated ecosystems store carbon dioxide partially as glycans, from which some have the potential to sequester carbon as a long-term storage. Especially the interaction of ecosystems makes it difficult to track carbon compounds back to their origin, resulting in difficulties budgeting their individual climate storage potential. Fucoidan might serve as a bioindicator for algal carbon stored in different locations. Overall, this study highlights the interplay and the interconnectedness of various ecosystems in storing large

amounts of carbon. Together they function as a key-nature based solution for marine carbon dioxide removal.

Methods

Sampling 50cm deep sediment cores were collected with a Russian peat corer (5cm diameter) in saltmarsh, seagrass, mangroves and unvegetated areas around the German Bight, Malaysia and Columbia (**Fig. 1A-C**). Up to 3 points per ecosystem were sampled along a transect (**Fig. 1D**), in total 93 cores were analysed (**Table S1**). Additionally, porewater samples were taken using lances or digging of holes. Samples were taken between 30 and 50 cm along 9 points per ecosystem at North Sea sites (**Table S2**). Samples were directly filtered over pre-combusted (450°C, 4.5h) GMF and GF/F filters and 200 ml of filtered porewater samples were frozen at -20°C for polysaccharide analysis.

Processing Cores were split visually according to physiochemical layers into up to 5 parts. Each layer was homogenized by hand in a ziplock bag and stored at 4°C. Subsamples were frozen at -20°C prior to freeze drying with an Alpha 1-4 LSCbasic freeze dryer from Christ at -55°C until constant vacuum. Samples were pulverised with a ball mill (FRITSCH LLC Planeten-Mikromühle PULVERISETTE 7 premium line) at 500 rpm for 3 min. Sediment powder was stored at room temperature in the dark until further analysis.
Porewater samples were run over AMICON filtration device with 5kDa membrane (Biomax) to separate the polysaccharide fraction over 5 kDa, washed 2 times with 300 µL MilliQ and up-concentrated by a factor of 5 in MilliQ-water. Samples were freeze dried and resuspended at a final concentration factor of 100 times in MilliQ-water.

Carbohydrate extraction 90 mg of dried and pulverised material was sequentially extracted using MilliQ-water and 0.3 M EDTA. Sediment was mixed with 1.8 mL of MilliQ-water, vortexed and kept in an ultrasonic water bath for 1 hour. Extracts were centrifuged at 6000G for 15 min.

The resulting supernatant was transferred into a new vial and the pellets were mixed with 1.8 mL of 0.3 M EDTA, vortexed and kept in an ultrasonic water bath for 1 hour. Extracts were centrifuged at 6000G for 15 min and the supernatant was again transferred into a new vial. Extracts were frozen at -20° until further analysis.

Phenol-sulfuric assay The total carbohydrate content was determined by mixing 100 µL of resuspended samples or extracts with 100 µL of 5% phenol solution and 500 µL of concentrated sulfuric acid, then incubate for 10 minutes at RT and afterwards for 20 min at 30°C. Absorbance at 490 nm was measured using Spectramax Id3 plate reader (Molecular Devices) against a glucose standard curve.

Acid hydrolysis Polysaccharides were acid hydrolysed into quantifiable monosaccharides by adding 300 µL 2M HCl to 300 µL of the porewater extracts and MilliQ-sediment extracts and the 20x diluted EDTA sediment extract in pre-combusted glass vials (450°C, 4.5 h). Glass vials were sealed and polysaccharides hydrolysed at 100°C for 24 h. The samples were transferred after hydrolysis to microtubes and dried in an acid-resistant vacuum concentrator (Martin Christ Gefriertrocknungsanlagen GmbH, Germany). Samples were resuspended in 300 µL MilliQ-water.

Monosaccharide quantification As previously described in two studies (20, 37), monosaccharides were quantified using anion exchange chromatography with pulsed amperometric detection (HPAEC-PAD). The sample analysis was conducted on a Dionex ICS-5000+ system, equipped with a CarboPac PA10 analytical column (2 x 250 mm) and a CarboPac PA10 guard column (2 x 50 mm). Neutral and amino sugars were separated applying an isocratic phase using 18 mM NaOH. A gradient reaching up to 200 mM $NaCH_3COO$ was applied to separate acidic monosaccharides.

Microarray MilliQ-water and EDTA sediment extracts were equally combined, 30 µL were transferred into wells of 384-microwell plates, where two consecutive two-fold dilutions were done in printing buffer (55.2% glycerol, 44% water, 0.8% Triton X-100). The microwell plates were centrifuged at 3500 x g for 10 min at 15 °C. Microarray printing and probing was performed as previously described in a recent study (26).

ELISA Polysaccharide were detected using enzyme-linked immunosorbent assay (ELISA) as described in the following studies (20, 38). In short, 100 µl of each combined sediment extract and the porewater samples were pipetted into a pre-coated 96 well plate and incubated overnight at 4°C. Signal was developed using primary antibodies (BAM1 for porewaters samples and BAM1 and JIM13 for sediment samples) in skim milk PBS solution at a concentration of 1:10, followed by antibody anti-rat in skim milk PBS solution at a concentration of 1:1000. Absorbance after development was measured at 450 nm using Spectramax Id3 plate reader (Molecular Devices).

Statistical analysis All statistical analysis were carried out using R4.4.1 (R core team, (39)) and Julia (40). The relative abundance of each monosaccharide was determined, all samples with a relative abundance of acidic sugars of over 50% were excluded from calculations. Pairwise distances were calculated using the Bray-Curtis distance metric for non-metric multidimensional scaling, using the vegan package (41). As NMDS can be quite sensitive to noise (42), we also applied diffusion maps (43) as a nonlinear dimensionality reduction method for comparison using 1/Bray-Curtis distance to construct the similarity matrix and a threshold of 5. The eigenvectors corresponding to the smallest non-zero eigenvalues are the most interesting as they identify the directions of the largest variation, i.e. the main dimensions of the data manifolds.

To test for significant changes between ecosystems combining MiliQ-water and EDTA extracts we applied the following statistical methods using the car package (44). In case of no normal distribution, we performed the Kruskal-Wallis test, followed by the pairwise Wilcoxon test with

α-correction according to Bonferroni to adjust for the inflation of type I error due to multiple testing. Bonferroni adjustment was performed as follows: p= 0.05/k, with k as the number of single hypotheses. Here, k= 6 was used for comparison among all 4 ecosystems and k= 3 for locations without mangroves. Therefore, α= 0.0083 or α= 0.0167 was considered statistically significant. When normality was met, we conducted an ANOVA, followed by a post-hoc Tukey test for pairwise comparisons.

Acknowledgments

The authors thank technicians at Max-Planck Institute for Marine Microbiology and Marum Centre for Environmental Research, University of Bremen, namely Tina Horstmann for assistance with carbohydrate microarray analysis, Katharina Föll for HPAEC-PAD measurements, as well as Theresa Fett and Mirco Wölfelschneider from Leibniz Centre for Tropical Marine Research (ZMT), Bremen, Germany for sampling of cores and processing of sediment cores. The authors thank Dariya Baiko and Michael Seidel from Institute for Chemistry and Biology of the Marine Environment (ICBM), Carl von Ossietzky Universität, Oldenburg and Jana Geuer and Tomasz Markowski from Max-Planck Institute for Marine Microbiology for sampling and processing of porewater. The authors thank José Ernesto Mancera-Pineda from Universidad Nacional de Colombia, Esteban Zarza González from Universidad del Sinú, Colombia, Jen Nie Lee from Faculty of Science and Marine Environment, Universiti Malaysia Terengganu and A. Aldrie Amir from Institute for Environment and Development (LESTARI), Universiti Kebangsaan Malaysia. Collections along the German North Sea coast in Lower Saxony and Schleswig-Holstein were made under the permit issued by the Lower Saxony Wadden Sea National Park Authority (Ref.no.: 01.2-22249-1-1.1 (60-8) / 2022) and the National Park Administration of the State Agency for Coastal Protection, National Park and Marine Conservation Schleswig-Holstein (Ref.no.: 3141-537.46) respectively. Collections along the German Baltic Sea coast near Massholm, Wendtorf, and Heiligenhafen were made under the permits issued by the Schleswig-Flensburg

District Department for Environment Section for Nature Conservation, the Plön District Administrator, Lower Nature Conservation Authority, Office for the Environment (Ref.no.: 3106-3/127/0161), and the District Administrator Department Nature and Soil (Ref.no.: 6.20.2-3117-IV-22-Fr) respectively. Collections from Colombia along the peninsula of Barú were made under the permit from the Sub-Directorate for Management and Administration of Protected Areas (Ref.no.: 20222000120371). Collections from Malaysia were made under permit from the Ministry of Natural Resources, Environment and Climate Change (Access and benefit-sharing, Ref 974126). The permission to carry out research in Kilim Geoforest Park (Forest Reserve) in Kedah, Malaysia was obtained and approved by the Director-General of the Forestry Department of Peninsular Malaysia (Reference No.: JH/ 100 Jld. 33 (75)). The permit to enter Kilim Geoforest Park (Forest Reserve) in Kedah, Malaysia was obtained from the Langkawi District Forest Office (Permit No.: KL 72.2022). The authors acknowledge invaluable support from the Max-Planck-Society, the sea4SoCiety, CDRmare campaign in the German Marine Research Alliance.

Author contributions

I.H. and J.-H.H. designed research with contributions from all authors; I.H. performed sampling in Germany and total carbohydrate, monosaccharide quantification and ELISA antibody binding. A.A.M. performed microarray analysis. I.H. and J.M. analyzed data and I.H. and J.H.H. led the manuscript production with contributions from all authors.

The authors declare no competing interest.

References

1. Temmink RJM *et al. (*2022) Recovering wetland biogeomorphic feedbacks to restore the world's biotic carbon hotspots. *Science (New York, N.Y.)* 376:eabn1479.
2. Mcleod E *et al. (*2011) A blueprint for blue carbon: toward an improved understanding of the role of vegetated coastal habitats in sequestering CO 2. *Frontiers in Ecol & Environ* 9:552–560.

3. Hagger V, Waltham NJ, Lovelock CE (2022) Opportunities for coastal wetland restoration for blue carbon with co-benefits for biodiversity, coastal fisheries, and water quality. *Ecosystem Services* 55:101423.

4. Gattuso J-P *et al. (*2018) Ocean Solutions to Address Climate Change and Its Effects on Marine Ecosystems. *Front. Mar. Sci.* 5.

5. Mengis N, Paul A, Fernández-Méndez M (2023) Counting (on) blue carbon—Challenges and ways forward for carbon accounting of ecosystem-based carbon removal in marine environments. *PLOS Clim* 2:e0000148.

6. Sogin EM *et al. (*2022) Sugars dominate the seagrass rhizosphere. *Nature ecology & evolution* 6:866–877.

7. Abdullah MI, Fredriksen S (2004) Production, respiration and exudation of dissolved organic matter by the kelp Laminaria hyperborea along the west coast of Norway. *J. Mar. Biol. Ass.* 84:887–894.

8. Wada S, Hama T (2013) The contribution of macroalgae to the coastal dissolved organic matter pool. *Estuarine, Coastal and Shelf Science* 129:77–85.

9. Wada S *et al. (*2007) Quantitative and qualitative analyses of dissolved organic matter released from Ecklonia cava Kjellman, in Oura Bay, Shimoda, Izu Peninsula, Japan. *Journal of Experimental Marine Biology and Ecology* 349:344–358.

10. Reed DC *et al. (*2015) Patterns and controls of reef-scale production of dissolved organic carbon by giant kelp Macrocystis pyrifera. *Limnology & Oceanography* 60:1996–2008.

11. Paine ER, Schmid M, Boyd PW, Diaz-Pulido G, Hurd CL (2021) Rate and fate of dissolved organic carbon release by seaweeds: A missing link in the coastal ocean carbon cycle. *Journal of phycology* 57:1375–1391.

12. Krause-Jensen D *et al. (*2018) Sequestration of macroalgal carbon: the elephant in the Blue Carbon room. *Biology letters* 14.

13. Krause-Jensen D, Duarte CM (2016) Substantial role of macroalgae in marine carbon sequestration. *Nature Geosci* 9:737–742.

14. Kennedy H *et al. (*2010) Seagrass sediments as a global carbon sink: Isotopic constraints. *Global Biogeochemical Cycles* 24.

15. Almahasheer H *et al. (*2017) Low Carbon sink capacity of Red Sea mangroves. *Scientific reports* 7:9700.

16. Ortega A *et al. (*2019) Important contribution of macroalgae to oceanic carbon sequestration. *Nat. Geosci.* 12:748–754.

17. Wada S *et al. (*2008) Bioavailability of macroalgal dissolved organic matter in seawater. *Mar. Ecol. Prog. Ser.* 370:33–44.

18. Watanabe K *et al. (*2020) Macroalgal metabolism and lateral carbon flows can create significant carbon sinks. *Biogeosciences* 17:2425–2440.

19. Filbee-Dexter K, Wernberg T (2020) Substantial blue carbon in overlooked Australian kelp forests. *Scientific reports* 10:12341.

20. Vidal-Melgosa S *et al. (*2021) Diatom fucan polysaccharide precipitates carbon during algal blooms. *Nature communications* 12:1150.

21. Buck-Wiese H *et al. (*2023) Fucoid brown algae inject fucoidan carbon into the ocean. *Proceedings of the National Academy of Sciences of the United States of America* 120:e2210561119.

22. Arnosti C, Fuchs BM, Amann R, Passow U (2012) Contrasting extracellular enzyme activities of particle-associated bacteria from distinct provinces of the North Atlantic Ocean. *Frontiers in microbiology* 3:425.

23. Lloyd CC *et al. (*2022) Particles act as 'specialty centers' with expanded enzymatic function throughout the water column in the western North Atlantic. *Frontiers in microbiology* 13:882333.

24. Giljan G *et al. (*2023) Selfish bacteria are active throughout the water column of the ocean. *ISME communications* 3:11.

25. Huang G *et al. (*2021) Secretion of sulfated fucans by diatoms may contribute to marine aggregate formation. *Limnology & Oceanography* 66:3768–3782.

26. Vidal-Melgosa S *et al. (*2022) *Not digested: algal glycans move carbon dioxide into the deep-sea*.

27. Salmeán AA, Willats WGT, Ribeiro S, Andersen TJ, Ellegaard M (2022) Over 100-Year Preservation and Temporal Fluctuations of Cell Wall Polysaccharides in Marine Sediments. *Frontiers in plant science* 13:785902.

28. Pante E, Simon-Bouhet B (2013) marmap: A package for importing, plotting and analyzing bathymetric and topographic data in R. *PloS one* 8:e73051.

29. Bivand RS (2021) Progress in the R ecosystem for representing and handling spatial data. *J Geogr Syst* 23:515–546.

30. Hellige I (2024) Algal-derived carbon transported into coastal vegetated ecosystems. Created in BioRender. *https://BioRender.com/x10y435.*

31. Aluwihare LI, Repeta DJ, Chen RF (1997) A major biopolymeric component to dissolved organic carbon in surface sea water. *Nature communications*:166–169.

32. Aluwihare LI, Repeta DJ, Chen RF (2002) Chemical composition and cycling of dissolved organic matter in the Mid-Atlantic Bight. *Deep Sear Research*.

33. Bligh M *et al. (*2024) Selective preservation of fucose-rich oligosaccharides in the North Atlantic Ocean. *bioRxiv*.

34. Koch H *et al. (*2019) Biphasic cellular adaptations and ecological implications of Alteromonas macleodii degrading a mixture of algal polysaccharides. *The ISME journal* 13:92–103.

35. Engel A, Thoms S, Riebesell U, Rochelle-Newall E, Zondervan I (2004) Polysaccharide aggregation as a potential sink of marine dissolved organic carbon. *Nature*:929–932.

36. Iversen MH (2023) Carbon Export in the Ocean: A Biologist's Perspective. *Annual Review of Marine Science*.

37. Engel A, Händel N (2011) A novel protocol for determining the concentration and composition of sugars in particulate and in high molecular weight dissolved organic matter (HMW-DOM) in seawater. *Marine Chemistry* 127:180–191.

38. Cornuault V, Manfield IW, Ralet M-C, Knox JP (2014) Epitope detection chromatography: a method to dissect the structural heterogeneity and inter-connections of plant cell-wall matrix glycans. *The Plant journal : for cell and molecular biology* 78:715–722.

39. R Core Team (2020) *R: A Language and Environment for Statistical Computing. R Foundation Stat. Computing (Vienna, Austria)*.

40. Bezanson J, Edelman A, Karpinski S, Shah VB (2017) Julia: A fresh approach to numerical computing. *SIAM Review*:65–98.

41. Oksanen J *et al. (*2018) Vegan: community ecology package. R package version 2.5.3. https://CRAN.R-project.org/package=vegan.

42. Fahimipour AK, Gross T (2020) Mapping the bacterial metabolic niche space. *Nature communications* 11:4887.

43. Coifman RR *et al. (*2005) Geometric diffusions as a tool for harmonic analysis and structure definition of data: Diffusion maps. *Proceedings of the National Academy of Sciences of the United States of America*:7426–7431.

44. Fox J *et al. (*2019) *car: Companion to Applied Regression*.